



# Benzo-Fused Perylene Oligomers with up to 13 Linearly Annulated Rings

Xuan Yang, Frank Rominger, and Michael Mastalerz\*

**Abstract:** The longer acenes with more than six linearly fused six-membered rings are still fascinating chemists and physicists because of their unique photophysical properties and their high potential for organic electronics applications. Unfortunately, with increasing size (seven and more rings) these compounds rapidly lose chemical stability. Besides kinetic and chemical stabilization approaches introducing either bulky or electron-withdrawing groups or both, such systems also have been stabilized by *peri*-annulation. Although strictly spoken, these *peri*-annulated compounds are no longer real acenes, they have fascinating properties as well. Herein, we describe the first synthesis of a new series of *peri*-annulated acenes with up to 13 linearly fused rings, which is unprecedented till date. Furthermore, this new series contains perylene units connected through benzene rings along their [b,k]edges, responsible for unique absorption and emission properties.

## Introduction

The larger acenes are a fascinating class of polycyclic aromatic hydrocarbons (PAHs) due to their distinct and unique photophysical, electrochemical and materials properties making them potentially superior candidates for organic electronics applications, such as for the construction of organic field effect transistors (OFETs).<sup>[1]</sup> It is known that for the larger acenes (five and more rings) the reactivity and thus instability is increasing significantly with the number of annulated rings.<sup>[1a]</sup> Despite the fact that even non-substituted acenes with up to eleven or twelve fused rings have been generated by matrix isolation experiments or on Au (111) surfaces,<sup>[2,3]</sup> the synthesis of soluble congeners of the same size in reasonable amounts is still lacking due to the intrinsic reactivity by photodegradation.<sup>[4]</sup> To the best of our knowledge the largest acene described is a nonacene, containing a number of bulky triisopropylsilyl ethynyl (TIPS)-substituents as well as electron-withdrawing fluoro substituents to prevent

it from rapid dimerization or degradation by photooxidation.<sup>[5]</sup>

The increasing instability of acenes with increasing number of rings can simply be explained by the heuristic Clar sextet rule, by which the drawing of just one sextet in each acene molecule is allowed, independent from the overall number of rings. Thus, the aromatic or benzenoid character and therefore stability is significantly decreased with increasing size. To overcome this problem, larger acenes have also been formally stabilized by *peri*-annulation (Figure 1).<sup>[6]</sup> Although these are strictly not anymore considered to be acenes in the classical sense, these compounds have also distinct and interesting photophysical properties. Typical examples for these *peri*-stabilized “acenes” are for example, pyrene-fused PAHs or those with one or two triphenylene units at the peripheries<sup>[6,7]</sup> of the acene backbone. To the best of our knowledge, the largest linearly fused PAH described to date consists of twelve annulated six-membered rings and is based on three pyrene units connected with each other by two anthracene moieties.<sup>[7b]</sup>

In 2016, our research group introduced a four-step synthetic route to a series of diarenoperylenees starting from 2,6-di-*tert*-butylantracene.<sup>[9]</sup> Key-steps were the twofold iridium-catalyzed borylation of the corresponding 9,10-dihydroanthracene followed by cross-coupling reactions with various aromatic ortho-bromoaldehydes and subsequent condensation, allowing to quickly generate a large number of soluble diarenoperylenees in large enough quantities to study their photophysical properties, feasibility for OFETs. Furthermore, the easy and scalable reactions allowed us to use the diarenoperylenees as molecular building blocks for the

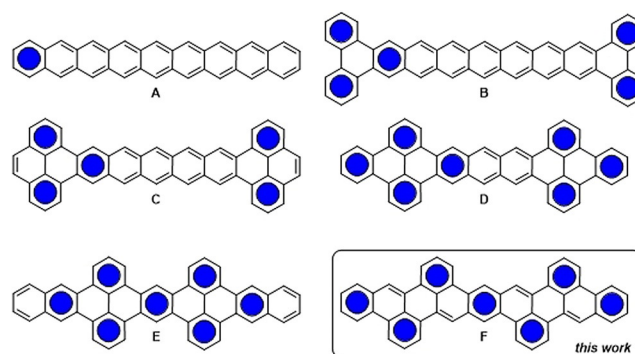


**Figure 1.** Structural comparison of nonacene (A) and *peri*-condensed nonacenes (B–F) and their heuristic Clar sextet (filled blue circles). Please note, that synthesis of substituted derivatives of A,<sup>[5a]</sup> B,<sup>[6]</sup> and C<sup>[8]</sup> have been described before. To the best of our knowledge, PAHs based on  $\pi$ -scaffolds D and E are still unknown.

[\*] Dr. X. Yang, Dr. F. Rominger, Prof. Dr. M. Mastalerz  
Organisch-Chemisches Institut, Ruprecht-Karls-Universität Heidelberg

Im Neuenheimer Feld 270, 69120 Heidelberg (Germany)  
E-mail: michael.mastalerz@oci.uni-heidelberg.de

Supporting information and the ORCID identification number(s) for the author(s) of this article can be found under:  
<https://doi.org/10.1002/anie.202017062>.

© 2021 The Authors. *Angewandte Chemie International Edition* published by Wiley-VCH GmbH. This is an open access article under the terms of the Creative Commons Attribution Non-Commercial License, which permits use, distribution and reproduction in any medium, provided the original work is properly cited and is not used for commercial purposes.

synthesis of cata-condensed heteroannulated coronenes or azulene-embedded PAHs.<sup>[10]</sup>

Herein, we now describe the synthesis of a small series of perylene-base PAHs with up to 13 linearly annulated rings based on the same type of reaction. To the best of our knowledge, this is the longest linearly fused purely hydrocarbon-based PAH described to date.<sup>[1a,b,11]</sup> It is worth mentioning that this type of  $\pi$ -framework has prior been used as one of the model structures by Risko and co-workers to investigate band gaps and predict charge carrier mobilities of polyacenes with different edge topologies by theoretical calculations.<sup>[12]</sup>

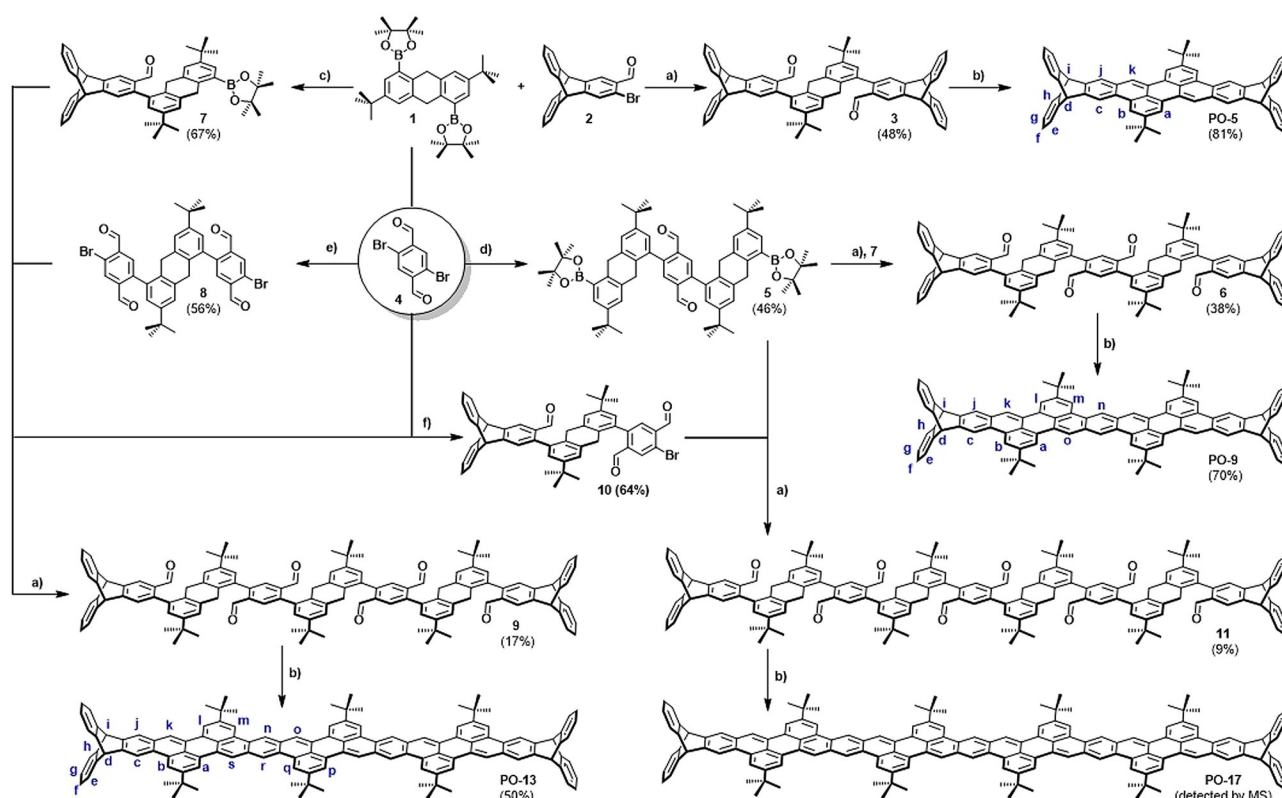
## Results and Discussion

### Synthesis and Characterization

To ensure a certain solubility especially of the larger members of this series we adopted the triptycene end-capping strategy, which was used before for larger fused aromatics and dyes.<sup>[13]</sup> In this respect, the smaller congener **PO-5** (Scheme 1) was synthesized by the same method as described before for a dibenzoperylene by Suzuki–Miyaura cross-coupling reaction of diboronic ester **1**<sup>[9]</sup> and triptycene based bromo aldehyde **2** under Fu conditions<sup>[14]</sup> giving dialdehyde **3** in 48% yield, which was converted to the yellow **PO-5** in 81% yield

by intramolecular condensation with *t*-BuOK. For **PO-9**, diboronic ester **5** was needed as the key intermediate. By applying Suzuki–Miyaura cross-coupling reaction between diboronic ester **1** and 2,5-dibromoterephthalaldehyde **4** in a molar ratio of 6:1 it was isolated in 46% yield. Note that here 10 mol% of Pd(PPh<sub>3</sub>)<sub>4</sub> was used as the catalyst. The isolated double coupled product was found to be deborylated when the reaction was performed under Fu conditions. Subsequent reaction of **5** with bromo aldehyde **2** gave tetraaldehyde precursor **6** in 38% isolated yield. As for **PO-5**, the last step is the condensation mediated by *t*-BuOK, which gave **PO-9** in 70% yield. It is worth to mention that in this case no silica gel column chromatography was needed for purification. The synthesis of **PO-13** is based on the same strategy using iterative Suzuki–Miyaura cross-coupling reactions. To achieve this, diboronic ester **1** was reacted with **4** in a stoichiometry of 6:1, to give monoboronic ester **7** in 67% yield. Another key substrate (**8**) was obtained in 56% yield by the reaction of diboronic ester **1** and dibromide **4** in a molar ratio of 1:6. Cross-coupling reaction between the two intermediates **7** and **8** resulted in the hexaaldehyde precursor **9** in 17% yield. Treatment with *t*-BuOK in hot THF gave **PO-13** as a dark-red solid in 50% yield. All compounds were fully characterized by NMR, (HR)-MS, IR, UV/Vis and emission spectroscopy (for details, see Supporting Information).

By MALDI mass spectra, the clean formation of **PO-5** ( $m/z = 816.37$ ), **PO-9** ( $m/z = 1202.57$ ) and **PO-13** ( $m/z = 1588.78$ )



**Scheme 1.** Synthesis of perylene oligomers **PO-5**, **PO-9** and **PO-13** a) 10 mol% Pd<sub>2</sub>(dba)<sub>3</sub>, 15 mol% *t*-Bu<sub>3</sub>PHBF<sub>4</sub>, K<sub>2</sub>CO<sub>3</sub> (aq.), THF, 80°C, 16 h; b) *t*-BuOK, THF, 60°C, 16 h; c) 5 mol% Pd(PPh<sub>3</sub>)<sub>4</sub>, K<sub>2</sub>CO<sub>3</sub> (aq.), THF, 80°C, 16 h, ratio of **1** to **2** is 6:1; d) 10 mol% Pd(PPh<sub>3</sub>)<sub>4</sub>, K<sub>2</sub>CO<sub>3</sub> (aq.), THF, 80°C, 16 h, ratio of **1** to **4** is 6:1; e) 10 mol% Pd(PPh<sub>3</sub>)<sub>4</sub>, K<sub>2</sub>CO<sub>3</sub> (aq.), THF, 80°C, 16 h, ratio of **1** to **4** is 1:6; f) 5 mol% Pd(PPh<sub>3</sub>)<sub>4</sub>, K<sub>2</sub>CO<sub>3</sub> (aq.), THF, 80°C, 16 h, ratio of **7** to **4** is 1:6.

is supported (Figure 2).  $^1\text{H}$  NMR spectra of these perylene oligomers were obtained in  $(\text{CDCl}_2)_2$  or  $o\text{-DCB-}d_4$  (**PO-13**) at room temperature (Figure 3), giving more detailed structural information. Whereas for **PO-5**, all signals are very sharp and well-resolved, for the longer **PO-9**, the peaks of the protons  $\text{H}^i\text{-H}^n$  are somewhat broadened. **PO-13**, is of significant lower solubility despite the two triptycene end-caps and the  $^1\text{H}$  NMR spectrum needed to be recorded in  $o\text{-DCB-}d_4$ .

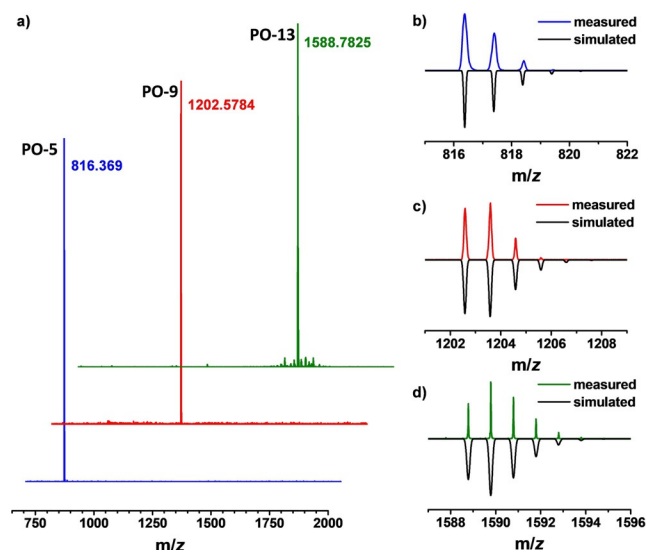


**Figure 2.** a) MALDI-TOF MS of **PO-5** (blue) and MALDI HRMS of **PO-9** (red) and **PO-13** (green). b–d) Comparisons of measured and simulated isotopic distribution patterns of **PO-5** (b), **PO-9** (c) and **PO-13** (d).

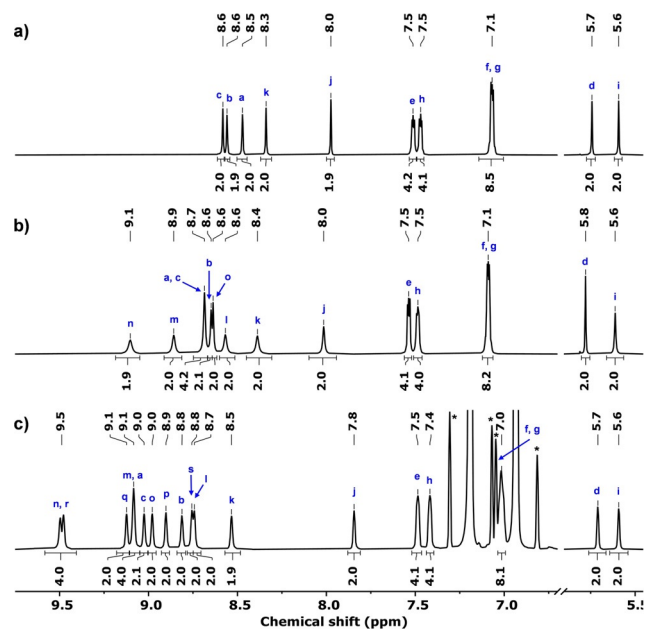


**Figure 3.** Partial  $^1\text{H}$  NMR spectra of a) **PO-5** (600 MHz, 298 K,  $\text{Cl}_2\text{CDCDCl}_2$ ); b) **PO-9** (600 MHz, 298 K,  $\text{Cl}_2\text{CDCDCl}_2$ ) and c) **PO-13** (700 MHz, 298 K,  $o\text{-DCB-}d_4$ ). For full spectra see Supporting Information. Peak assignments are according to those of the molecular structures in Scheme 1. \*Satellite peaks of  $o\text{-DCB}$ .

Despite the low solubility the signals are well-resolved, suggesting that no dimer or oligomer formation in solution at 1.0 mM concentration occurs. A pronounced appearance of the most inner protons (eg.)  $\text{H}^n$  in **PO-9** and **PO-13** in the downfield area of the spectra may give a hint on delocalization of  $\pi$ -electrons and the related (overall) diamagnetic ring-current (vide infra).

We also attempted the synthesis of **PO-17** with 17 linearly annulated rings by a similar strategy. Therefore, monoboronic ester **7** was reacted with an excess of dibromodialdehyde **4** to give **10** in 64% yield. Subsequent twofold cross-coupling delivered octalaldehyde **11** in 9% yield after tedious separation with recycling GPC. Unfortunately, any conditions we tried for the base-mediated cyclization to convert **11** to **PO-17** gave never pure material. Although a main peak of the objected **PO-17** (monoisotopic signal of  $m/z = 1975.209$ ) was found by mass spectrometry a large number of other peaks suggesting that in competition to the desired condensation reactions, partially Cannizzarro disproportionation<sup>[15]</sup> to carboxylate and benzylic alcohol groups occurred (Figure S51). This is supported by two new peaks at  $1692\text{ cm}^{-1}$  ( $\text{C}=\text{O}$  stretching) and  $1060\text{ cm}^{-1}$  ( $\text{C}-\text{O}$  stretching of  $-\text{CH}_2\text{OH}$ ) in the FTIR spectrum (Figure S44). All attempts to purify **PO-17** by recycling-GPC, recycling-HPLC, precipitation or recrystallization unfortunately failed. We used for example various bases such as *t*-BuOK, KOH, NaOH,  $\text{Cs}_2\text{CO}_3$ ,  $\text{Et}_3\text{N}$ ; various solvents, such as toluene, benzene,  $\text{CH}_2\text{Cl}_2$  or 1,4-dioxane; different temperatures or concentrations, but either **PO-17** was not generated properly or the formation of Cannizzarro products could not be avoided in any of these cases. It is worth mentioning, that this phenomenon was also observed during the synthesis of **PO-13**. However, here these impurities were minor and could still be removed by recrystallization.

Single crystals of **PO-9** suitable for X-ray diffraction analysis were obtained by vapor diffusion of *n*-hexane into a  $\text{CH}_2\text{Cl}_2$  solution (Figure 4). **PO-9** crystallizes in the triclinic space group  $P\bar{1}$  with three (disordered)  $\text{CH}_2\text{Cl}_2$  molecules in the asymmetric unit. The data quality is high enough, allowing a detailed analysis of C–C bond lengths. The two six-membered rings with the *tert*-butyl groups show the smallest bond-length alternation, considering that these have the most benzenoid character. The longest bonds (1.46–1.47 Å) are found at the central ring of the perylene unit, somewhat disconnecting the two halves of the perylene  $\pi$ -systems, similar as found for perylene itself or other fused perylene compounds.<sup>[9,16]</sup> As found before for smaller structures, the red-highlighted bonds are with 1.36–1.37 Å relatively short and exhibit more olefinic character.<sup>[9]</sup> According to these data, the  $\pi$ -electronic structure can be best described as stabilized by seven Clar sextets (Figure 4b). **PO-9** molecules arrange in an offset coplanar fashion with an average distance of 4.96 Å between the “nonacene”  $\pi$ -planes (Figure 4c & d). Thus, as objected, the two triptycene end-caps suppress efficient  $\pi$  stacking.<sup>[13]</sup>

All perylene oligomers were investigated by absorption and emission spectroscopy (Figure 3 and Table 1). Well-resolved  $\beta$ - and  $p$ -band ( $\pi\text{-}\pi^*$  transitions) absorptions were observed for all POs. The absorption maximum at the longest wavelength bathochromically shifts from 449 nm for **PO-5** to

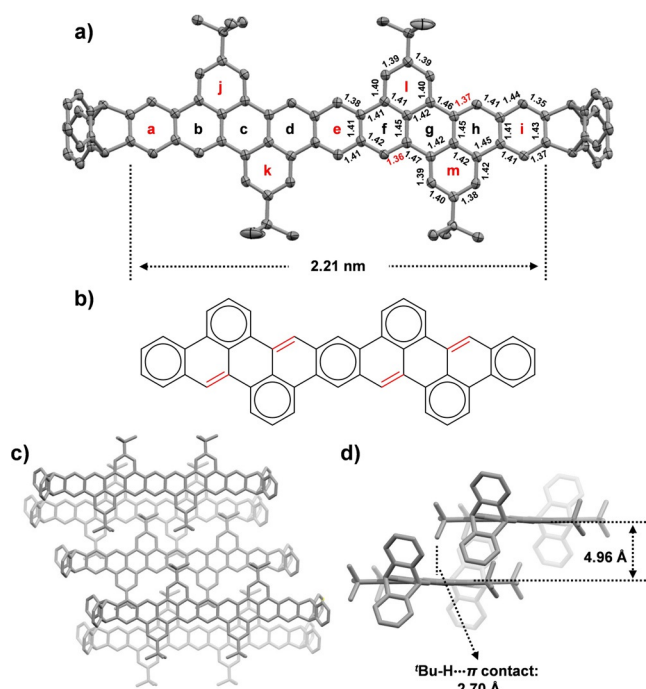


**Figure 4.** Single crystal X-ray structure of **PO-9** (a, c and d). a) ORTEP plot with thermal ellipsoids set at 50% probability and C–C bond lengths in Å. Shortest bonds are highlighted in red. b) Molecular structure of **PO-9** according to Clar's rule. Isolated C–C double bonds are highlighted in red. (c and d) Packing. Hydrogen atoms as well as enclathrated solvent molecules have been omitted for clarity.

510 nm for **PO-9** and 534 nm for **PO-13**. Especially the *p*-band transitions have for each compound distinct vibronic patterns, suggesting that these are relative stiff in solution. By increasing molecular length of the POs, the optical band gap decreases from 2.7 eV for **PO-5** to 2.4 eV for **PO-9** to 2.2 eV for **PO-13**. This trend is supported by DFT calculated energy levels of frontier molecular orbitals (Table 1 and Supporting Information).

The POs show a strong and colorful emission in chloroform. Whereas **PO-5** emits at  $\lambda_{em,1} = 462$  nm with a bright blue color, **PO-9** is green ( $\lambda_{em,1} = 523$  nm) and **PO-13** yellow ( $\lambda_{em,1} = 549$  nm) (Figure 5). According to the difference of emission and fluorescence, the Stokes shifts are relatively small between  $\tilde{\nu} = 487$  and  $627$   $\text{cm}^{-1}$ . It is worth mentioning that the quantum yield efficiencies for all compounds are very high, especially for the longer systems **PO-9** ( $\Phi = 86\%$ ) and **PO-13** ( $\Phi = 83\%$ ), which may be a result from the stiffness of the backbone in combination with a low tendency of self-aggregation.<sup>[13a]</sup>

**Table 1:** Summary of the photophysical properties and DFT calculations.

Compd.	$\lambda_{max}$ [nm] <sup>[a,b]</sup>	$E_g^{opt}$ [eV] <sup>[a,c]</sup>	$\lambda_{em}$ ( $\lambda_{ex}$ ) [nm] <sup>[a,b]</sup>	$\tilde{\nu}$ [ $\text{cm}^{-1}$ ] <sup>[e]</sup>	$\Phi$ [%] <sup>[f]</sup>	$\tau$ [ns] <sup>[g]</sup>	$E_{HOMO}$ [eV] <sup>[h]</sup>	$E_{LUMO}$ [eV] <sup>[h]</sup>
<b>PO-5</b>	449	2.7	462, 494, 530 (422)	627	68 ± 3	2.1	−5.03	−1.95
<b>PO-9</b>	510	2.4	523, 562, 610 (475)	487	86 ± 1	1.5	−4.88	−2.23
<b>PO-13</b>	534	2.2	549, 591, 645 (499)	512	83 ± 1	1.4	−4.83	−2.34

[a] Measured in chloroform at room temperature ( $c = 2\text{--}13 \times 10^{-6}$  M). [b] Absorption maximum at the longest wavelength. [c] Estimated from absorption onset. [d] Emission maxima. [e] Stokes shift. [f] Fluorescence quantum yield. [g] Fluorescence lifetime. [h] Calculated by DFT at the B3LYP/6-311G(d) level.

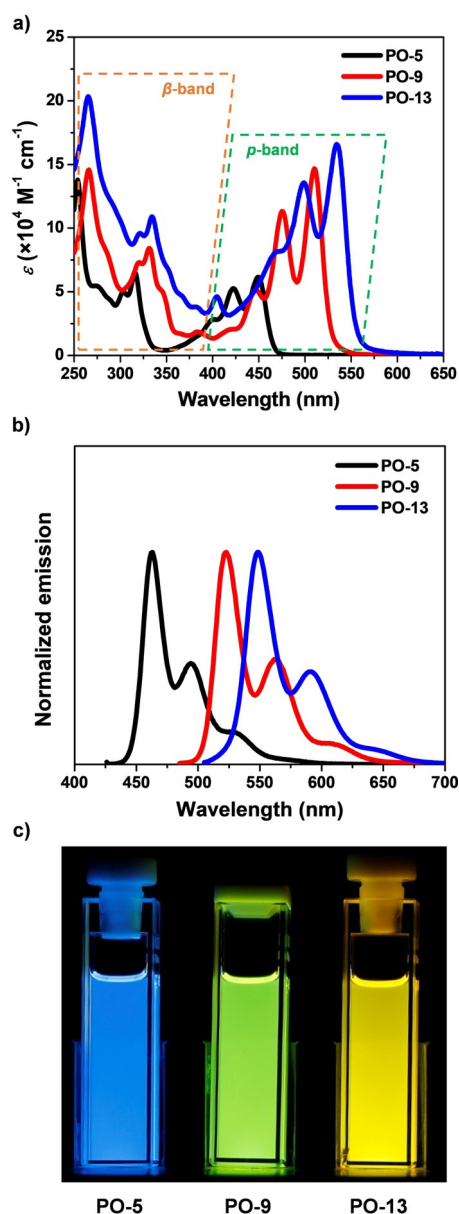


**Figure 5.** a) UV/Vis absorption and b) emission spectra of all POs measured in chloroform at room temperature. c) Optical images of POs in chloroform ( $c = 5.0 \times 10^{-6}$  M) under irradiation at 366 nm.

DFT calculated NICS(1) values (Figure 6)<sup>[17]</sup> of all three compounds revealed that the central rings of each perylene unit shows no diamagnetic ring-current (NICS(1) = +1.2 for each ring). This is basically supported by the ACID-plots considering the contribution of  $\pi$ -electrons exclusively

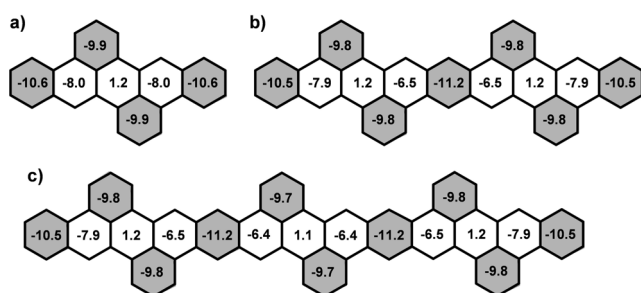


**Figure 6.** DFT calculated NICS(1) values of **PO-5** (a), **PO-9** (b) and **PO-13** (c) at the B3LYP/6-31G(d) level. The triptycene end-caps are omitted for clarity.

(Figure 7).<sup>[18]</sup> By both methods, it is suggested that chromophoric units (phenanthrene and dibenzo[*a,h*]anthracene) are electronically separated. However, there must be some contribution of electronic communication between these chromophoric units, explaining the increasing bathochromic shifts of the *p*-bands in the UV/vis spectra with increasing molecular length, which is different from for example, another oligomeric series of pyrene-fused pyrazaacenes, where the absorption spectra do not qualitatively change with increasing length.<sup>[19]</sup> Similar observation has been made for pyrene based oligomeric PAHs.<sup>[20]</sup> However, DFT calculated frontier molecular orbitals reveal that for all POs, HOMOs and LUMOs are delocalized over the whole  $\pi$ -backbones (Figures S63–S65), which reflects the band-gap narrowing with increasing molecular size, responsible for the red-shift. This is supported by TD-DFT calculations (Figures S66–S68, Tables S1–S3).

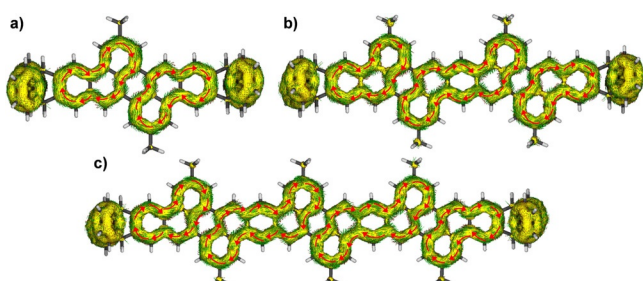


**Figure 7.** DFT calculated ACID plots for perylene oligomers **PO-5** (a), **PO-9** (b), **PO-13** (c) at the B3LYP/6-311G(d,p) level. The calculations only include the contributions from occupied  $\pi$ -orbitals. The isosurface value is 0.03 and the magnetic field points out of the paper plane. The diamagnetic (clockwise) ring currents are highlighted by red arrows.

## Conclusion

To summarize, a new series of discrete PAHs with up to 13 linearly annulated six-membered rings has been synthesized (**PO-5**, **PO-9** and **PO-13**), which is to the best of our knowledge the longest purely hydrocarbon based system of such kind. The incorporated perylene units are responsible for the unique photophysical properties, such as the very high quantum yield efficiencies for emission of > 80 % even for the

longest systems (**PO-13**). The synthetic strategy used herein namely cross-coupling of aromatic (di)bromo-(di)aldehydes followed by condensation reactions found its limit in the attempted synthesis of **PO-17**. Although the cross-coupled precursor was isolated, during condensation, a substantial number of side-products by Cannizzaro disproportionation occurred making the isolation of **PO-17** impossible. However, since **PO-17** is formed and was detected by MS, further endeavors are currently made in our lab to synthesize higher members of this fascinating new PAHs (or graphene nanoribbons)<sup>[21]</sup> and study their materials properties as well as their chemistry more detailed.

## Acknowledgements

X.Y. likes to thank the China Scholarship Council (CSC) for a PhD scholarship. The authors are grateful to the Deutsche Forschungsgemeinschaft (DFG) for financial support within the collaborative research center SFB 1249 (TP A04). Furthermore, we acknowledge support by the state of Baden Württemberg through bwHPC and the DFG through grant no INST 40/575 1 FUGG (JUSTUS 2 cluster). Open access funding enabled and organized by Projekt DEAL.

## Conflict of interest

The authors declare no conflict of interest.

**Keywords:** acenes · condensation · fluorescence · peri-annulation · polycyclic aromatic hydrocarbons

- [1] a) M. Müller, L. Ahrens, V. Brosius, J. Freudenberg, U. H. F. Bunz, *J. Mater. Chem. C* **2019**, *7*, 14011–14034; b) W. Chen, F. Yu, Q. Xu, G. Zhou, Q. Zhang, *Adv. Sci.* **2020**, *7*, 1903766; c) J. Li, S. Chen, Z. Wang, Q. Zhang, *Chem. Rec.* **2016**, *16*, 1518–1530; d) J. E. Anthony, *Angew. Chem. Int. Ed.* **2008**, *47*, 452–483; *Angew. Chem.* **2008**, *120*, 460–492; e) H. F. Bettinger, C. Tönshoff, *Chem. Rec.* **2015**, *15*, 364–369; f) H. F. Bettinger, *Pure Appl. Chem.* **2010**, *82*, 905–915.
- [2] a) B. Shen, J. Tatchen, E. Sanchez-Garcia, H. F. Bettinger, *Angew. Chem. Int. Ed.* **2018**, *57*, 10506–10509; *Angew. Chem.* **2018**, *130*, 10666–10669; b) H. F. Bettinger, R. Mondal, D. C. Neckers, *Chem. Commun.* **2007**, 5209–5211; c) R. Mondal, C. Tönshoff, D. Khon, D. C. Neckers, H. F. Bettinger, *J. Am. Chem. Soc.* **2009**, *131*, 14281–14289; d) C. Tönshoff, H. F. Bettinger, *Angew. Chem. Int. Ed.* **2010**, *49*, 4125–4128; *Angew. Chem.* **2010**, *122*, 4219–4222.
- [3] a) J. I. Urgel, S. Mishra, H. Hayashi, J. Wilhelm, C. A. Pignedoli, M. Di Giovannantonio, R. Widmer, M. Yamashita, N. Hieda, P. Ruffieux, H. Yamada, R. Fasel, *Nat. Commun.* **2019**, *10*, 861; b) F. Eisenhut, T. Kühne, F. García, S. Fernández, E. Guitián, D. Pérez, G. Trinquier, G. Cuniberti, C. Joachim, D. Peña, F. Moresco, *ACS Nano* **2020**, *14*, 1011–1017.
- [4] a) R. Einholz, H. F. Bettinger, *Angew. Chem. Int. Ed.* **2013**, *52*, 9818–9820; *Angew. Chem.* **2013**, *125*, 10000–10003; b) R. Einholz, T. Fang, R. Berger, P. Grüniger, A. Früh, T. Chassé, R. F. Fink, H. F. Bettinger, *J. Am. Chem. Soc.* **2017**, *139*, 4435–4442.
- [5] a) B. Purushothaman, M. Bruzek, S. R. Parkin, A.-F. Miller, J. E. Anthony, *Angew. Chem. Int. Ed.* **2011**, *50*, 7013–7017; *Angew.*

- Chem.* **2011**, *123*, 7151–7155; b) M. M. Payne, S. R. Parkin, J. E. Anthony, *J. Am. Chem. Soc.* **2005**, *127*, 8028–8029.
- [6] M. Müller, S. Maier, O. Tverskoy, F. Rominger, J. Freudenberg, U. H. F. Bunz, *Angew. Chem. Int. Ed.* **2020**, *59*, 1966–1969; *Angew. Chem.* **2020**, *132*, 1982–1985.
- [7] a) M. Müller, E. C. Rüdiger, S. Koser, O. Tverskoy, F. Rominger, F. Hinkel, J. Freudenberg, U. H. F. Bunz, *Chem. Eur. J.* **2018**, *24*, 8087–8091; b) H. M. Duong, M. Bendikov, D. Steiger, Q. Zhang, G. Sonmez, J. Yamada, F. Wudl, *Org. Lett.* **2003**, *5*, 4433–4436; c) J. Li, Y. Zhao, J. Lu, G. Li, J. Zhang, Y. Zhao, X. Sun, Q. Zhang, *J. Org. Chem.* **2015**, *80*, 109–113; d) D. Rodríguez-Lojo, D. Pérez, D. Peña, E. Guitián, *Chem. Commun.* **2015**, *51*, 5418–5420; e) M. Martínez-Abadía, G. Antonicelli, E. Zuccatti, A. Atxabal, M. Melle-Franco, L. E. Hueso, A. Mateo-Alonso, *Org. Lett.* **2017**, *19*, 1718–1721; f) D.-C. Huang, C.-H. Kuo, M.-T. Ho, B.-C. Lin, W.-T. Peng, I. Chao, C.-P. Hsu, Y.-T. Tao, *J. Mater. Chem. C* **2017**, *5*, 7935–7943; g) J. Xiao, C. D. Malliakas, Y. Liu, F. Zhou, G. Li, H. Su, M. G. Kanatzidis, F. Wudl, Q. Zhang, *Chem. Asian J.* **2012**, *7*, 672–675; h) W. Chen, X. Li, G. Long, Y. Li, R. Ganguly, M. Zhang, N. Aratani, H. Yamada, M. Liu, Q. Zhang, *Angew. Chem. Int. Ed.* **2018**, *57*, 13555–13559; *Angew. Chem.* **2018**, *130*, 13743–13747.
- [8] J. Xiao, H. M. Duong, Y. Liu, W. Shi, L. Ji, G. Li, S. Li, X.-W. Liu, J. Ma, F. Wudl, Q. Zhang, *Angew. Chem. Int. Ed.* **2012**, *51*, 6094–6098; *Angew. Chem.* **2012**, *124*, 6198–6202.
- [9] G. Zhang, F. Rominger, U. Zschieschang, H. Klauk, M. Mastalerz, *Chem. Eur. J.* **2016**, *22*, 14840–14845.
- [10] a) X. Yang, F. Rominger, M. Mastalerz, *Org. Lett.* **2018**, *20*, 7270–7273; b) X. Yang, M. Hoffmann, F. Rominger, T. Kirschbaum, A. Dreuw, M. Mastalerz, *Angew. Chem. Int. Ed.* **2019**, *58*, 10650–10654; *Angew. Chem.* **2019**, *131*, 10760–10764; c) X. Yang, F. Rominger, M. Mastalerz, *Angew. Chem. Int. Ed.* **2019**, *58*, 17577–17582; *Angew. Chem.* **2019**, *131*, 17741–17746.
- [11] a) G. Liu, C. Xiao, F. Negri, Y. Li, Z. Wang, *Angew. Chem. Int. Ed.* **2020**, *59*, 2008–2012; *Angew. Chem.* **2020**, *132*, 2024–2028; b) W. Fan, T. Winands, N. L. Doltsinis, Y. Li, Z. Wang, *Angew. Chem. Int. Ed.* **2017**, *56*, 15373–15377; *Angew. Chem.* **2017**, *129*, 15575–15579; c) T. J. Sisto, Y. Zhong, B. Zhang, M. T. Trinh, K. Miyata, X. Zhong, X. Y. Zhu, M. L. Steigerwald, F. Ng, C. Nuckolls, *J. Am. Chem. Soc.* **2017**, *139*, 5648–5651.
- [12] Q. Ai, K. Jarolimek, S. Mazza, J. E. Anthony, C. Risko, *Chem. Mater.* **2018**, *30*, 947–957.
- [13] a) B. Kohl, F. Rominger, M. Mastalerz, *Angew. Chem. Int. Ed.* **2015**, *54*, 6051–6056; *Angew. Chem.* **2015**, *127*, 6149–6154; b) B. Kohl, F. Rominger, M. Mastalerz, *Chem. Eur. J.* **2015**, *21*, 17308–17313; c) K. Baumgärtner, A. L. M. Chinchá, A. Dreuw, F. Rominger, M. Mastalerz, *Angew. Chem. Int. Ed.* **2016**, *55*, 15594–15598; *Angew. Chem.* **2016**, *128*, 15823–15827; d) B. P. Benke, L. Hertwig, X. Yang, F. Rominger, M. Mastalerz, *Eur. J. Org. Chem.* **2021**, 72–76.
- [14] M. R. Netherton, G. C. Fu, *Org. Lett.* **2001**, *3*, 4295–4298.
- [15] a) C. G. Swain, A. L. Powell, W. A. Sheppard, C. R. Morgan, *J. Am. Chem. Soc.* **1979**, *101*, 3576–3583; b) in *Name Reactions: A Collection of Detailed Reaction Mechanisms*, Springer Berlin Heidelberg, Berlin, **2006**, pp. 107–108; c) Z. Wang, *Comprehensive Organic Name Reactions and Reagents*, Wiley, Hoboken, **2010**, pp. 602–605.
- [16] M. Botoshansky, F. H. Herstein, M. Kapon, *Helv. Chim. Acta* **2003**, *86*, 1113–1128.
- [17] Z. Chen, C. S. Wannere, C. Corminboeuf, R. Puchta, P. v. R. Schleyer, *Chem. Rev.* **2005**, *105*, 3842–3888.
- [18] D. Geuenich, K. Hess, F. Köhler, R. Herges, *Chem. Rev.* **2005**, *105*, 3758–3772.
- [19] D. Cortizo-Lacalle, J. P. Mora-Fuentes, K. Strutyński, A. Saeki, M. Melle-Franco, A. Mateo-Alonso, *Angew. Chem. Int. Ed.* **2018**, *57*, 703–708; *Angew. Chem.* **2018**, *130*, 711–716.
- [20] K. Ozaki, K. Kawasumi, M. Shibata, H. Ito, K. Itami, *Nat. Commun.* **2015**, *6*, 6251.
- [21] J. Liu, X. Feng, *Angew. Chem. Int. Ed.* **2020**, *59*, 23386–23401; *Angew. Chem.* **2020**, *132*, 23591–23607.

Manuscript received: December 23, 2020

Revised manuscript received: January 18, 2021

Accepted manuscript online: January 18, 2021

Version of record online: February 26, 2021